

Small carbon clusters (C_n^0 , C_n^+ , C_n^-) from acyclic and cyclic precursors Neutralization–reionization and theory

Aberra Fura^{a,1}, František Tureček^{b,*}, Fred W. McLafferty^{a,2}

^a Baker Chemistry Laboratory, Cornell University, Ithaca, NY 14853-1301, USA

^b Department of Chemistry, University of Washington, P.O. Box 351700, Bagley Hall, Seattle, WA 98195-1700, USA

Received 10 August 2001; accepted 29 October 2001

Dedicated to the memory of Pierre Longevialle.

Abstract

Dissociative ionization of several linear, cyclic, and branched molecules was used to generate C_3^+ and C_4^+ carbon clusters. However, mass spectra from collisionally activated dissociation (CAD) and neutralization–reionization (NR) under a wide variety conditions were indistinguishable, indicating only one isomer or same mixture of isomers. Likewise, CAD and NR spectra of C_4^+ and C_3^+ from $^{13}CH_2=CH-CH=^{13}CH_2$ and $CH_3-^{13}C=CH_2$ show complete $^{12}C/^{13}C$ scrambling. CAD cross sections are consistent with $C_4^+-C_6^+$ ions as mainly linear isomers and C_7^+ ions from cyclic precursors as mainly cyclic. CCSD(T) ab initio and B3LYP density functional theory calculations with large basis sets yielded structures and energies for a variety of cationic, neutral, and anionic carbon clusters and transition states for some cationic rearrangements. The calculated enthalpies of formation, dissociation energies, ionization energies, and electron affinities mostly agree with currently accepted experimental data. However, CCSD(T) calculations indicate adiabatic ionization energies for C_3 (11.79 eV) and C_4 isomers (10.48, 10.82, and 10.86 eV) that differ >1 eV from recent measurements. (Int J Mass Spectrom 217 (2002) 81–96) © 2002 Elsevier Science B.V. All rights reserved.

Keywords: Carbon cluster; Collisionally activated dissociation; Neutralization–reionization

1. Introduction

Carbon clusters were first studied spectroscopically using emission from interstellar clouds and other cosmic environments [1,2]. As reviewed [3,4], the chemistry of C_n molecules and ions in plasmas (carbon arcs, laser ablation) [2,6] and in the formation

of polynuclear aromatics, diamond films [7], and soot [2,8] has been the subject of extensive theoretical and experimental research; the latter was mostly focused on ionic species, although spectroscopic studies of matrix-isolated neutral carbon clusters have been also reported [9]. Following our preliminary study [10], there have been recently reports on C_4 [11] and C_5 [12] neutral carbon clusters that were generated from linear anionic precursors using neutralization–reionization mass spectrometry (NR-MS) [13]. In this paper we report a detailed study of C_3 to C_6 carbon clusters generated from linear and

* Corresponding author.

E-mail: turecek@macmail.chem.washington.edu

¹ Present address: Bristol Myers Squibb, Princeton, NJ 08543-4000, USA.

² Co-corresponding author.

cyclic cationic precursors and analyzed by NRMS following conversion to anions and cations.

Theoretical calculations have predicted for small C_n^0 species that odd-numbered clusters have lower electron affinities, closed shell ground states, and higher stabilities. For the cationic C_n^+ counterparts, a similar order of stability was indicated, whereas for C_n^- anions an opposite trend was found [4,5,14–16]. Although stable C_n^0 and C_n^+ ($n < 10$) structures were first predicted to be non-cyclic, more recent ab initio calculations showed stability also for cyclic isomers [4,5,15] with the two isomers close in energy for C_3^+ [15,17], C_4 [15,18], and C_4^+ [15]. In addition, most recent high-level studies [19–23] have agreed on the existence of branched structures for C_4^0 , C_4^+ , and C_4^- species that were in general substantially less stable than the most stable linear or cyclic isomers.

In experimental studies, carbon vaporization, with and without post-photoionization, yielded mass spectra with more abundant odd-numbered C_n^+ and even-numbered C_n^- clusters [4,23–27] as predicted by theory. This is more indicative of the relative stabilities of C_n^+ and C_n^- than of C_n^0 . As pointed out for C_n^+ spectra by Bowers and co-workers [25], the actual C_n^0 abundances measured by mass spectrometry depend significantly on ionization cross sections and C_n^+ stabilities. However, the high relative stability of C_3^0 is supported by its preferential loss from both C_n^+ [4,25–27] and C_n^- [24]. Mass-selected C_n^+ clusters undergoing metastable [25], collisionally activated [26,27a], and laser dissociation [4] also favor formation of C_n^+ species of odd-numbered n values. Threshold dissociation energies of C_n^+ species were measured by collisionally activated dissociation (CAD) and showed the odd-numbered clusters to be more stable than the even-numbered ones up to $n = 9$, in qualitative agreement with theoretical predictions [15a].

Concerning isomeric characterization, evidence for open chain C_n^0 , C_n^+ , and C_n^- has come from photoelectron [28], infrared [29], microwave [2,30], and electron [9] spectroscopy, low-energy C_n^+ dissociations [25], and ion mobility values [31]. However,

stable cyclic structures are indicated for C_{4-6}^0 neutrals and C_3^+ ions by coulomb explosion techniques [32], and, from the same laboratory, for C_{3-7}^0 neutrals by electron affinity measurements [32c,33]. The latter values were much lower than those reported earlier [28], possibly because the cyclic isomers were present in <10% concentration [32c], with the admixture dependent on laser/graphite interaction conditions [33]. Almlöf and co-workers [29g] noted that the structures obtained in frozen inert gas matrices may differ from those in the gas phase [29h]. Additionally, cyclic C_3^+ was indicated by infrared spectra using an argon matrix [34], and a second, presumably cyclic, C_7^+ isomer by differences in bimolecular reactivity [27] and ion mobility [31]. All these studies utilized high-temperature formation from elemental carbon of these clusters, whose formation entropy should favor linear isomers [4].

In a different approach that could avoid the entropic preference, Lifshitz and co-workers [26] utilized dissociative electron ionization of cyclic perchlorinated molecules to generate C_n^+ with $n = 3, 5, 6, 7$, and ≤ 10 , but found no evidence that this method gave different isomeric structures than those generated by carbon vaporization. A more specific method of preparation of linear C_n^- anions was reported recently that utilized fluoride-induced desilylation of trimethylsilylated diyne precursors [11,12].

Here, we have extended the cationic approach in an attempt to prepare linear, branched, and cyclic C_n^+ ions. Of these, C_3^+ and C_4^+ were studied most extensively because their isomers are predicted to be stable and of closely similar energies [4,15–23]. Further, with NRMS [13], these mass-selected cations are then utilized to form the corresponding neutrals and anions. Product abundances from their competitive unimolecular dissociations are used to evaluate basic thermodynamic values proposed for C_n^0 , C_n^+ and C_n^- [4,5,35–37], for which major disagreements still exist. Additional theoretical calculations have been performed to guide these experiments.

2. Experimental

Using a tandem double-focusing (EB–EB, E = electrostatic, B = magnetic sector) mass spectrometer described in detail elsewhere [38], ions formed by 70 eV electrons were accelerated by 10 keV, mass selected by MS-I (EB), and underwent charge-exchange collisions with a neutral target gas in the first collision cell (Cl-I) to form fast neutrals. The calcium neutralization experiments employed a special furnace for vaporization temperatures up to 800°C and special care to minimize Hg background (a reason that Xe was used as a high IE target instead of Hg) [38b]. Residual ions were deflected electrostatically, and the fast neutrals were made to undergo collisional reionization in Cl-II to yield cations or anions. Negative ions were also formed by charge reversal of the precursor cations with benzene in Cl-II. The resulting ions were separated by kinetic energies in E-II and detected. For cross section values, the neutral beam flux was measured using a retractable channeltron multiplier at Cl-III before E-II. The designation $^+NR^+$, Na (85%T)/O₂ (70%T) indicates a spectrum from cation neutralization with Na at 85% precursor beam transmittance, followed by residual ion deflection (slash) and reionization to cations with O₂ at 70% beam transmittance. Data acquisition, reduction, and computer control employed a PC-based computer system [38c].

Specific ion precursors included: hexabromobenzene (*c*-C₆Br₆), hexachlorobenzene (*c*-C₆Cl₆), benzene (*c*-C₆H₆), hexachlorocyclopentadiene (*c*-C₅Cl₆), 1,3-butadiene (*n*-C₄H₆), hexachloro-1,3-butadiene (*n*-C₄Cl₆), 1,4-dibromo-2-butyne (*n*-C₄H₄Br₂), 1-bromo-2-methylpropene (*i*-C₄H₇Br), 1,2,-dibromo-2-methylpropane (*i*-C₄H₈Br₂), propene (*n*-C₃H₆), and cyclopropane (*c*-C₃H₆). H₂¹³C=CHCH=¹³CH₂ was synthesized adopting the procedure for the corresponding ¹⁴C-isotopomer [39]. All other compounds, including CH₂=¹³C–CH₃, were obtained commercially.

3. Calculations

Standard ab initio calculations were performed using the Gaussian 98 suite of programs [40].

Geometries were optimized with spin-unrestricted density functional theory calculations using Becke's hybrid functional (UB3LYP) [41], and the 6-311+G(2df) basis set. Stationary points were characterized by harmonic frequency calculations as local minima (all real frequencies) or first-order saddle points (one imaginary frequency). Improved energies were obtained by single-point calculations using B3LYP and Duning's triple- ζ correlation-consistent basis set furnished with diffuse functions, aug-cc-pVTZ [42]. In an additional set of calculations, single points were obtained by spin-unrestricted coupled-cluster calculations [43,44], using single, double, and perturbational triple excitations of valence electrons, UCCSD(T)/aug-cc-pVTZ. Spin contamination in the DFT calculations was low, as judged from the $\langle S^2 \rangle$ operator expectation values that were 0.75–0.77 for doublets, 2.00–2.02 for triplets, and 3.75–3.76 for quartets. Spin contamination in the UCCSD(T) calculations was largely reduced by annihilation of higher spin states through projection [45] that gave $\langle S^2 \rangle$ within 0.02 of those expected for pure spin states.

4. Results and discussion

4.1. Theoretical calculations of carbon cluster structures and energies

Although a large number of carbon clusters have been addressed by previous theoretical calculations [5,11,12,14–22], those were carried out at widely different levels of theory and are therefore difficult to unify to provide a coherent description of the systems under study here. Ab initio calculations of carbon clusters are notoriously difficult because of a multitude of bound electronic states for the singlet and triplet states in C_{*n*}⁰ and doublet and quartet states in C_{*n*}⁺ and C_{*n*}[–], and often necessitate the use of multireference configuration interaction methods to obtain the correct electronic state [46]. Density functional theory calculations tend to provide ground electronic states and are therefore useful for geometry optimization of carbon clusters. As a case in point, starting from the MRD-CI

Table 1
Optimized geometries and harmonic frequencies

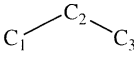
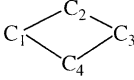
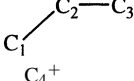
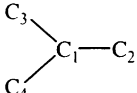
Species	Symmetry group	Electronic state	Geometry		Harmonic frequencies (cm ⁻¹) ^a
			Bond length (Å)	Bond angle (°)	
C ₁ –C ₂					
C ₂	<i>D</i> _{∞h}	¹ Σ _g ⁺	1.246		1873 (σ _g)
C ₂ ⁺	<i>D</i> _{∞h}	⁴ Σ _g ⁻	1.403		1334 (σ _g)
C ₂ ⁻	<i>D</i> _{∞h}	² Σ _g ⁺	1.258		1842 (σ _g)
C ₂ ⁻	<i>D</i> _{∞h}	⁴ Δ _u	1.427		1178 (σ _g)
C ₁ –C ₂ –C ₃					
C ₃	<i>D</i> _{∞h}	¹ Σ _g	1.287		135 (π _u), 135 (π _u), 1242 (σ _g), 2144 (σ _u)
C ₃	<i>C</i> _{∞v}	³ Π	C ₁ –C ₂ : 1.284 C ₂ –C ₃ : 1.296		235 (π), 397 (π), 484 (σ), 1223 (σ)
C ₃ ⁺	<i>D</i> _{∞h}	² Σ _u	1.287		100 (π _u), 100 (π _u), 1232 (σ _g)
C ₃ ⁺	<i>D</i> _{∞h} (<i>C</i> _{2v})	⁴ B ₁	1.263		277 (a ₁), 1345 (a ₁), 1915 (b ₂)
C ₃ ⁻	<i>D</i> _{∞h}	² Σ _g	1.301		277 (π _u), 419 (π _u), 1198 (σ _g), 1763 (σ _u)
C ₃ ⁻	<i>D</i> _{∞h} (<i>C</i> _{2v})	⁴ A ₂	1.306		445 (a ₁), 1172 (a ₁), 1521 (b ₂)
					
C ₃	<i>D</i> _{3h}	³ A' ₁	1.363	60	1168 (e'), 1168 (e'), 1614 (a' ₁)
C ₃ ⁺	<i>C</i> _{2v}	² B ₂	1.310	66.7	735 (a ₁), 1239 (b ₂), 1658 (a ₁)
C ₃ ⁺ (TS)	<i>C</i> _{2v}	² B ₂	1.288	136.0	i112 (a ₁), 1365 (a ₁), 2343 (b ₂)
C ₃ ⁺	<i>D</i> _{3h}	⁴ A' ₁	1.388	60	1182 (b ₂), 1182 (a ₁), 1554 (a ₁)
C ₃ ⁻	<i>C</i> _{2v}	² A ₁	1.356	68.8	773 (a ₁), 913 (b ₂), 1554 (a ₁)
C ₃ ⁻	<i>C</i> _{2v}	⁴ A ₂	1.369	70.1	278 (b ₂), 674 (a ₁), 1461 (a ₁)
C ₁ –C ₂ –C ₃ –C ₄					
C ₄	<i>D</i> _{∞h}	¹ Σ _g	C ₁ –C ₂ : 1.306 C ₂ –C ₃ : 1.290		150 (π _u), 212 (π _u), 302 (π _g), 489 (π _g), 939 (σ _g), 1603 (σ _u), 2125 (σ _g)
C ₄	<i>D</i> _{∞h}	³ Σ _g	C ₁ –C ₂ : 1.304 C ₂ –C ₃ : 1.286		178 (π _u), 178 (π _u), 385 (π _g), 385 (π _g), 942 (σ _g), 1597 (σ _u), 2123 (σ _g)
C ₄ ⁺	<i>D</i> _{∞h}	² Σ _u	C ₁ –C ₂ : 1.364 C ₂ –C ₃ : 1.254		113 (π _u), 148 (π _u), 259 (π _g), 335 (π _g), 891 (σ _g), 1323 (σ _u), 2140 (σ _g)
C ₄ ⁻	<i>D</i> _{∞h}	² Π _g	C ₁ –C ₂ : 1.270 C ₂ –C ₃ : 1.333		222 (π _u), 243 (π _u), 445 (π _g), 515 (π _g), 923 (σ _g), 1775 (σ _u), 2097 (σ _g)
					
C ₄	<i>D</i> _{2h}	¹ A _g	C ₁ –C ₂ : 1.442 C ₂ –C ₄ : 1.493	C ₁ –C ₂ –C ₃ : 117.6 C ₂ –C ₃ –C ₄ : 62.4	312 (b _{3u}), 502 (b _{2u}), 949 (a _g), 1013 (b _{3g}), 1285 (b _{1u}), 1391 (b _{1u})
C ₄	<i>C</i> _{2v}	³ A	C ₁ –C ₂ : 1.434 C ₂ –C ₄ : 1.435	C ₁ –C ₂ –C ₃ : 85.8 C ₂ –C ₃ –C ₄ : 85.7	616 (a), 640 (a), 641 (a), 704 (b), 711 (b), 1316 (a)
C ₄ ⁺	<i>C</i> _s	² A'	C ₁ –C ₂ : 1.370 C ₂ –C ₃ : 1.491	C ₁ –C ₂ –C ₃ : 11.3 C ₂ –C ₁ –C ₄ : 71.8	317 (a'), 422 (a'), 569 (a''), 1101 (a'), 1203 (a'), 1309 (a')
C ₄ ⁻	<i>D</i> _{2h}	² B _{2g}	C ₁ –C ₂ : 1.448 C ₂ –C ₄ : 1.457	C ₁ –C ₂ –C ₃ : 119.6 C ₂ –C ₃ –C ₄ : 60.4	121 (b _{3g}), 485 (b _{2u}), 513 (b _{3u}), 996 (a _g), 1208 (b _{1u}), 1308 (a _g)
					
C ₄ ⁺	<i>C</i> _{2v}	⁴ B ₁	C ₁ –C ₂ : 1.275 C ₂ –C ₃ : 1.305	C ₁ –C ₂ –C ₃ : 149.9	217 (a ₁), 452 (a ₂), 512 (b ₂), 1064 (a ₁), 1934 (a ₁), 2114 (b ₂)

Table 1 (Continued)

Species	Symmetry group	Electronic state	Geometry		Harmonic frequencies (cm ⁻¹) ^a
			Bond length (Å)	Bond angle (°)	
 C ₄	C _s	¹ A''	C ₁ –C ₂ : 1.326 C ₁ –C ₃ : 1.485 C ₁ –C ₄ : 1.412	C ₂ –C ₁ –C ₃ : 140.3 C ₂ –C ₁ –C ₄ : 162.5	79 (a'), 237 (a'), 696 (a'), 871 (a'), 1298 (a'), 1673 (a')
C ₄	C _{3v}	³ A ₁	C ₁ –C ₂ : 1.387	C ₂ –C ₁ –C ₃ : 108.0 C ₄ –C ₁ –C ₂ –C ₃ : 116.6	199 (e), 199 (e), 337 (a ₁), 1090 (e), 1090 (e), 1173 (a ₁)
C ₄ ⁺ (TS)	C _{2v} (C _s)	² A ₁	C ₁ –C ₂ : 1.377 C ₁ –C ₃ : 1.430 C ₃ –C ₄ : 1.413	C ₂ –C ₁ –C ₃ : 150.4	i1112 (b ₂), 276 (b ₁), 300 (b ₂), 786 (a ₁), 1195 (a ₁), 1479 (a ₁)
C ₄ ⁺	C _{2v}	⁴ A ₂	C ₁ –C ₂ : 1.377 C ₁ –C ₃ : 1.433 C ₃ –C ₄ : 1.311	C ₂ –C ₁ –C ₃ : 152.8	230 (b ₂), 340 (b ₁), 839 (a ₁), 851 (b ₂), 1328 (a ₁), 1689 (a ₁)

^aUncorrected B3LYP/6-311+G(2df) frequencies.

geometry for ground-state C₂⁺ [46], our B3LYP optimization yielded the ⁴Σ_g⁻ ground state of the ion, and likewise ground-state geometries of desired spin multiplicity were obtained for other species. The optimized geometries, electronic state assignments, and harmonic frequencies are summarized in Table 1.

Three local minima were found for C₃⁰, e.g., the linear singlet and triplet, and a cyclic triplet of which (¹Σ_g)C₃⁰ is by far the most stable neutral structure (Table 2). In line with previous studies [17a,20] we obtained a cyclic (²B₂) and linear (²Σ_u) structure for C₃⁺ of very similar energies (Table 3). A transition state for C₃⁺ isomer interconversion was found to be only 5 kJ/mol above the less stable linear isomer, indicating an extremely facile isomerization. For C₃⁻, the linear doublet (²Π_g) is the by far most stable structure, followed by the cyclic doublet (²A₁), while the quartet structures are substantially less stable.

Linear, cyclic, and branched structures were found to be local minima for the singlet and triplet states of C₄⁰ (Table 1) in keeping with previous studies [5,11,15]. The cyclic singlet is the most stable C₄⁰ isomer, followed closely by the linear triplet which is only 6 kJ/mol less stable from our CCSD(T) calculations. The branched singlet and triplet structures

are pyramidized at the central carbon atom. We find the electron configuration for the branched singlet to be ¹A'' as opposed to ¹A' reported previously from B3LYP calculations with a smaller basis set.

We found two local minima for doublet C₄⁺, e.g., the most stable cyclic isomer of C_s symmetry and the linear isomer. This order of stability was reversed

Table 2
Relative energies of neutral carbon clusters

Structure	Symmetry group	Electronic state	Relative energy ^a	
			B3LYP ^b	CCSD(T) ^b
C ₄ ⁰				
Cyclic	C _{2h}	¹ A _g	0	0
Linear	D _{∞h}	¹ Σ _g	5	43
Branched	C _s	¹ A''	91	112
Cyclic	D _{∞h}	³ Σ _g	-70	6
Linear	C _{2v}	³ A	108	115
Branched	C _{3v}	³ A ₁	403	365
C ₃ ⁰				
Linear	D _{∞h}	¹ Σ _g	0	0
Cyclic	D _{3h}	³ A' ₁	80	86
Linear	D _{∞h}	³ Π _g	204	222

^aAt 0 K in units of kJ/mol.

^bCalculations with the aug-cc-pVTZ basis set including B3LYP/6-311+G(2df) zero-point corrections.

in B3LYP calculations that made the linear isomer 26 kJ/mol more stable. At our level of theory, the slightly puckered C_s structure for cyclic C_4^+ was lower in energy than the planar C_{2v} structure reported recently [11]. In addition, we find branched C_4^+ structures (C_s or C_{2v}) to be first-order saddle points with one imaginary frequency (Table 1). The energy of the C_{2v} saddle point (2A_1 state) relative to the most stable cyclic C_4^+ isomer ($\Delta E = 108$ kJ/mol) was substantially lower than for the 2B_1 state reported as a local minimum ($\Delta E = 169$ kJ/mol) by Blanksby et al. [11]. These differences may be due to the different basis sets used to find the stationary points, which was 6-31G(d) in [11] and 6-311+G(2df) in the present work. Nevertheless, the existence of a local energy minimum for the lower-energy branched doublet structure appears to be in doubt. We found no low-lying local energy minimum for linear quartet C_4^+ , which was a saddle point for degenerate isomerization of a bent C_{2v} structure. The latter is another low-energy isomer that is calculated to be only 62 kJ/mol above (${}^2A'$) C_4^+ . In addition, we found a branched quartet C_4^+ to be a local energy minimum (Table 1) which was 119 kJ/mol above the most stable cyclic doublet C_4^+ isomer (Table 3).

Table 3
Relative energies of cationic carbon clusters

Structure	Symmetry group	Electronic state	Relative energy ^a	
			B3LYP ^b	CCSD(T) ^b
C_4^+				
Cyclic	C_s	${}^2A'$	0	0
Linear	$D_{\infty h}$	${}^2\Pi_g$	-24	10
Branched ^c	C_{2v}	2A_1	99	108
Linear ^c	$D_{\infty h}$	4X	25	
Bent	C_{2v}	4B_1	22	62
Branched	C_{2v}	4A_2	86	119
C_3^+				
Cyclic	C_{2v}	2B_2	0	0
Linear	$D_{\infty h}$	${}^2\Sigma_u$	34	4
TS	C_{2v}	2B_2	35	5
Cyclic	D_{3h}	${}^4A'_1$	31	58
Linear	$D_{\infty h}$ (C_{2v})	(4B_1)	130	169

^aAt 0 K in units of kJ/mol.

^bCalculations with the aug-cc-pVTZ basis set including B3LYP/6-311+G(2df) zero-point corrections.

^cFirst-order saddle points.

Table 4
Relative energies of anionic carbon clusters

Structure	Symmetry group	Electronic state	Relative energy ^a	
			B3LYP ^b	CCSD(T) ^b
C_4^-				
Linear	$D_{\infty h}$	${}^2\Pi_g$	0	0
Cyclic	D_{2h}	${}^2B_{2g}$	167	125
Linear	$D_{\infty h}$	${}^4\Delta_u$	269	278
C_3^-				
Linear	$D_{\infty h}$	${}^2\Pi_g$	0	0
Cyclic	C_{2v}	2A_1	58	43
Linear	$D_{\infty h}$ (C_{2v})	(4A_2)	130	169
Cyclic	C_{2v}	4B_1	309	293

^aAt 0 K in units of kJ/mol.

^bCalculations with the aug-cc-pVTZ basis set including B3LYP/6-311+G(2df) zero-point corrections.

Linear doublets were the most stable structures for both C_3^- and C_4^- (Tables 1 and 4). Cyclic doublets and quartet structures were also found as local minima but were substantially less stable than the linear doublets.

4.2. Carbon cluster electron affinities and ionization energies

The structures and energies for the most stable neutral and ionic isomers allowed us to calculate the pertinent adiabatic ionization energies and electron affinities that were compared with experimental data (Table 5) and further used to evaluate ion dissociation energies (Table 6). The electron affinities show very good agreement with experimental data for C [47], C_2 [48,49] and C_3 [48,50,51], where the CCSD(T) data are within 0.04–0.08 eV of accurate values from photoelectron spectra of anions. Interestingly, the calculated EAs for C_4 allow us to reinterpret the photoelectron spectrum of C_4^- reported by Neumark and co-workers [48]. The main low-energy peak in the spectrum (corresponding to EA = 3.882 eV) agrees very well with the calculated electron affinity of the linear triplet, (${}^3\Sigma_g^-$) C_4 (3.82 eV, Table 5). A less intense peak (corresponding to EA = 4.173 eV) that was assigned by Neumark and co-workers to (${}^1\Delta_g$) C_4^0 , coincides with our calculated electron affinity of

Table 5
Ionization energies and electron affinities of carbon clusters

Neutral	Ion	Energy ^{a,b}			Reference
		B3LYP/aug-cc-pVTZ	CCSD(T)/aug-cc-pVTZ	Experimental	
(³ P)C	(² P)C ⁺	11.54	11.18	11.26	[35]
(³ P)C	(⁴ S)C ⁻	1.37	1.22	1.263	[35,47]
(1Σ _g ⁺)C ₂	(4Σ _g ⁻)C ₂ ⁺	11.79	11.80	11.92	[53]
				11.41	[52]
				12.15	[54]
				3.273	[48]
(1Σ _g ⁺)C ₂	(2Σ _g ⁺)C ₂ ⁻	4.36	3.18	3.265	[49]
				3.265	[49]
(1Σ _g)C ₃	(2Σ _u)C ₃ ⁺	12.22	11.79	12.97	[57]
				11.1	[55]
				12.1	[56]
				–	
(³ Π _g)C ₃	(² Σ _u)C ₃ ⁺	10.10	9.49	–	
(³ A ₁)C ₃	(² B ₂)C ₃ ⁺	11.03	10.86	–	
(1Σ _g)C ₃	(2Π _g)C ₃ ⁻	2.20	1.95	1.995	[48]
				1.981	[50]
				1.950	[51]
(1Σ _g)C ₄	(2Π _g)C ₄ ⁺	10.48	10.48	12.54	[57]
(1A _g)C ₄	(2A')C ₄ ⁺	10.81	10.82	–	
(³ Σ _g)C ₄	(2Π _g)C ₄ ⁺	11.25	10.86	–	
(1Σ _g)C ₄	(2Π _g)C ₄ ⁻	4.50	4.20	4.173	[48]
				3.73	[48]
(3Σ _g)C ₄	(2Π _g)C ₄ ⁻	3.73	3.82	3.882	[48]
				3.70	[51]
(1A _g)C ₄	(2B _{2g})C ₄ ⁻	2.69	2.45	–	

^aAt 0 K adiabatic values in units of electron volt (eV).

^bElectron affinities given as positive values.

(1Σ_g⁺)C₄⁰ (4.20 eV, Table 5). The preferential formation of (³Σ_g⁻)C₄⁰ upon photoionization of (2Π_g)C₄⁻ is not due to Franck–Condon effects, because the equilibrium structures of (1Σ_g⁺) and (³Σ_g⁻)C₄⁰ are very similar. Rather, the peak intensities in the photoelectron spectrum were affected by energy-dependent electron detection efficiency. The most stable cyclic isomer, (1A_g)C₄⁰, is calculated to have a substantially lower electron affinity (2.45 eV) and was not observed in the photoionization measurements [48].

The calculated ionization energies are in good agreement with experimental data for C₁ [35] and C₂ [52–54]. The IE for C₃⁰ is bracketed by the values from older measurements [55,56], but substantially lower than the more recent datum of Ramathan et al. [57] (Table 5). We note that ionization of linear C₃⁰

to the most stable bent isomer of C₃⁺ is likely to face substantial Franck–Condon effects which may influence the experimental measurements. The calculated ionization energies of C₄⁰ span 10.48–10.86 eV depending on the neutral isomer (Table 5). These values are substantially smaller than the single experimental determination by Ramathan et al. (12.54 eV [57]). The reason for this discrepancy is unclear.

4.3. Isomer characterization for CAD and NR spectra

CAD (O₂ (50%T)) of 10 keV C₂⁺–C₇⁺ clusters gave the spectra shown in Fig. 1 that were in agreement with the CAD (air) spectra of 8 keV C₃⁺, C₅⁺, C₆⁺, and C₇⁺ ions [26,27a]. However, our C₃⁺ and C₄⁺

Table 6
Dissociation energies of carbon clusters

Reaction	Relative energy ^a		
	B3LYP ^b	CCSD(T) ^b	Experimental ^c
C_n⁰			
$(^1\Sigma_g^+)C_2 \rightarrow (^3P)C + (^3P)C$	503	588 ^d	605
	505	591 ^d	
$(^1\Sigma_g)C_3 \rightarrow (^3P)C + (^1\Sigma_g^+)C_2$	829	843 ^d	838
		698	697
$(^1A_g)C_4 \rightarrow (^3P)C + (^1\Sigma_g)C_3$	447	700	734
		461	490
$(^1A_g)C_4 \rightarrow 2(^1\Sigma_g^+)C_2$	788	467	566
		585	582
		591	705
$C_5^0 \rightarrow C_1^0 + C_4^0$	–	–	682
$C_5^0 \rightarrow C_2^0 + C_3^0$	–	–	567
$C_6^0 \rightarrow C_1^0 + C_5^0$	–	–	480
$C_6^0 \rightarrow C_2^0 + C_4^0$	–	–	557
$C_6^0 \rightarrow C_3^0 + C_3^0$	–	–	350
C_n^{+e}			
$(^4\Sigma_g^-)C_2^+ \rightarrow (^3P)C + (^2P)C^+$	551	525	542
$(^2B_2)C_3^+ \rightarrow (^3P)C + (^4\Sigma_g^-)C_2^+$	735	692	680
$(^2B_2)C_3^+ \rightarrow (^2P)C^+ + (^1\Sigma_g^+)C_2$	798	644	616
$(^2A')C_4^+ \rightarrow (^3P)C + (^2B_2)C_3^+$	548	550	448
$(^2A')C_4^+ \rightarrow (^2P)C^+ + (^1\Sigma_g)C_3$	517	496	367
$(^2A')C_4^+ \rightarrow (^4\Sigma_g^-)C_2^+ + (^1\Sigma_g^+)C_2$	796	669	522
C_n^{-e}			
$(^2\Sigma_g^+)C_2^- \rightarrow (^4S)C^- + (^3P)C$	777	763	799
$(^2\Pi_g)C_3^- \rightarrow (^4S)C^- + (^1\Sigma_g^+)C_2$	909	768	768
$(^2\Pi_g)C_3^- \rightarrow (^2P)C + (^2\Sigma_g^+)C_2^-$	620	579	574
$(^2\Pi_g)C_4^- \rightarrow (^4S)C^- + (^1\Sigma_g)C_3$	741	705	743
$(^2\Pi_g)C_4^- \rightarrow (^2P)C + (^2\Pi_g)C_3^-$	661	635	672
$(^2\Pi_g)C_4^- \rightarrow (^1\Sigma_g^+)C_2 + (^2\Sigma_g^+)C_2^-$	793	640	641
$C_5^- \rightarrow C_1^0 + C_4^-$	–	–	581
$C_5^- \rightarrow C_1^- + C_4^0$	–	–	834
$C_5^- \rightarrow C_2^0 + C_3^-$	–	–	649
$C_5^- \rightarrow C_2^- + C_3^0$	–	–	526
$C_6^- \rightarrow C_1^0 + C_5^-$	–	–	610
$C_6^- \rightarrow C_1^- + C_5^0$	–	–	762
$C_6^- \rightarrow C_2^0 + C_4^-$	–	–	586
$C_6^- \rightarrow C_2^- + C_4^0$	–	–	646
$C_6^- \rightarrow C_3^- + C_3^0$	–	–	562

^aIn units of kJ/mol.

^bCalculations with the aug-cc-pVTZ basis set including B3LYP/6-311+G(2df) zero-point corrections.

^cAt 0 K values in upper lines from [37], 298.15 K values in lower lines from the NIST database [35].

^dAt 0 K relative energies in upper lines, 298.15 K relative energies in lower lines.

^eAt 0 K relative energies for cations and anions.

CAD spectra were independent ($\pm 10\%$) of the wide variety of precursor molecules used. Further, these spectra were not significantly changed by collisionally activating (He (50%T), first field-free region) the

precursor ions to increase their internal energy. The CAD spectra of C_6^+ from *c*- C_6Cl_6 and *c*- C_6Br_6 , and of C_7^+ from toluene and cycloheptatriene were also closely similar.

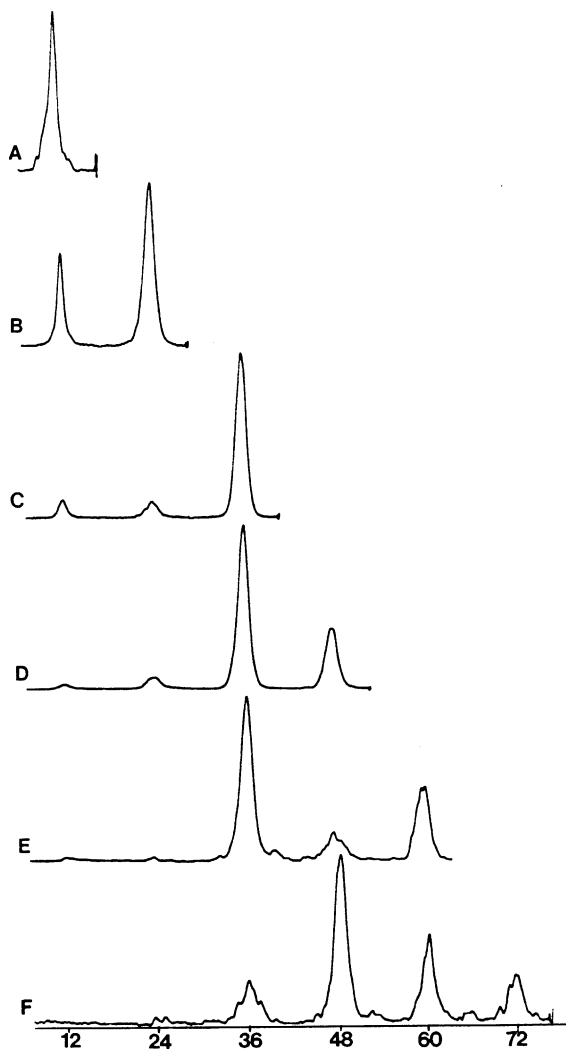


Fig. 1. CAD spectra, O₂ (50%T), identical ($\pm 10\%$) for the same ion from the listed precursors: (A) C₂⁺ from *n*-C₃H₆, *n*-C₄Cl₆; (B) C₃⁺ from *n*-C₃H₆, *n*-C₄Cl₆, *c*-C₃H₆, *c*-C₅Cl₆; (C) C₄⁺ from *n*-C₄H₆, *n*-C₄H₄Br₂, *n*-C₄Cl₆, *i*-C₄H₈, *i*-C₄H₇Br, *i*-C₄H₈Br₂, *c*-C₅Cl₆, *c*-C₆H₆, and *c*-C₆Cl₆; (D) C₅⁺ from *c*-C₅Cl₅; (E) C₆⁺ from *c*-C₆Cl₆ and *c*-C₆Br₆; (F) C₇⁺ from toluene and cycloheptatriene.

NR mass spectra have been used successfully to differentiate a multiplicity of isomers for cations whose CAD spectra were closely similar, such as those of C₄H₈ and C₄H₄ [58]. However, our NRMS studies with the wide variety of C_{*n*}⁺ precursors (Figs. 2 and 3) found no isomeric differences outside experimental

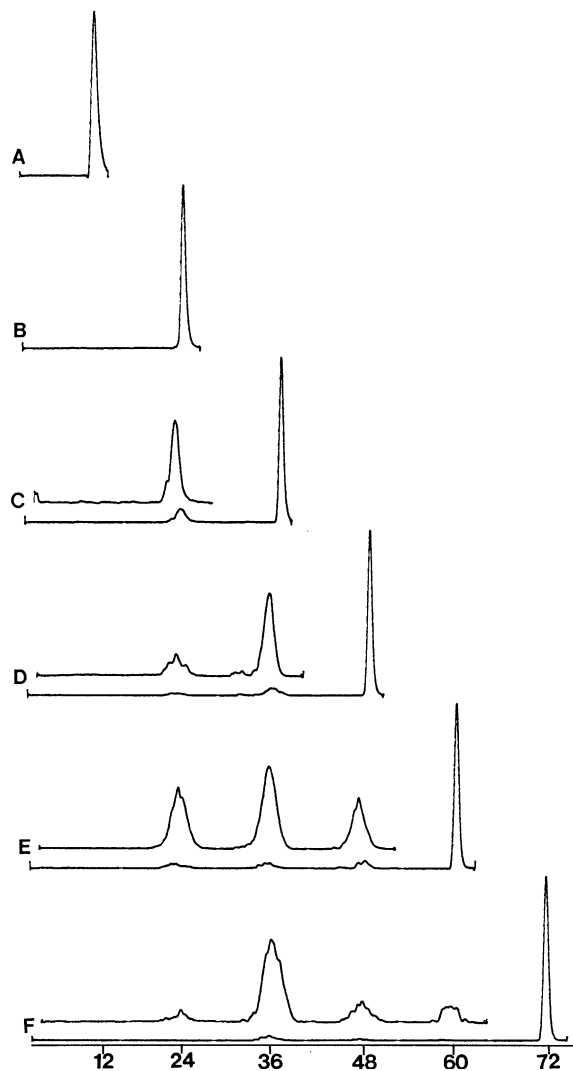


Fig. 2. Charge reversal ⁺NR⁻ spectra, C₆H₆ (30%T), identical ($\pm 20\%$) for the same ion from the listed precursors: (A–F) C₁⁺–C₆⁺, respectively, as in Fig. 1, except C₄⁺ is from *n*-C₄Cl₆, *i*-C₄H₇Br, and *c*-C₅Cl₆. Higher trace is amplified 10-fold.

error. The C_{*n*}⁺ charge-exchange spectra (⁺NR⁻ C₆H₆ (30%T), Fig. 2) gave similar ($\pm 20\%$) data for C₃⁺ and C₄⁺, irrespective of the precursor used, and this was also true ($\pm 10\%$) for neutralization of C_{*n*}⁺ with Xe, Na, or K followed by reionization (O₂ (70%T), Fig. 3).

All C_{*n*}⁺ spectra from neutralization with xenon (70%T, IE = 12.1 eV) are dominated by the reionized

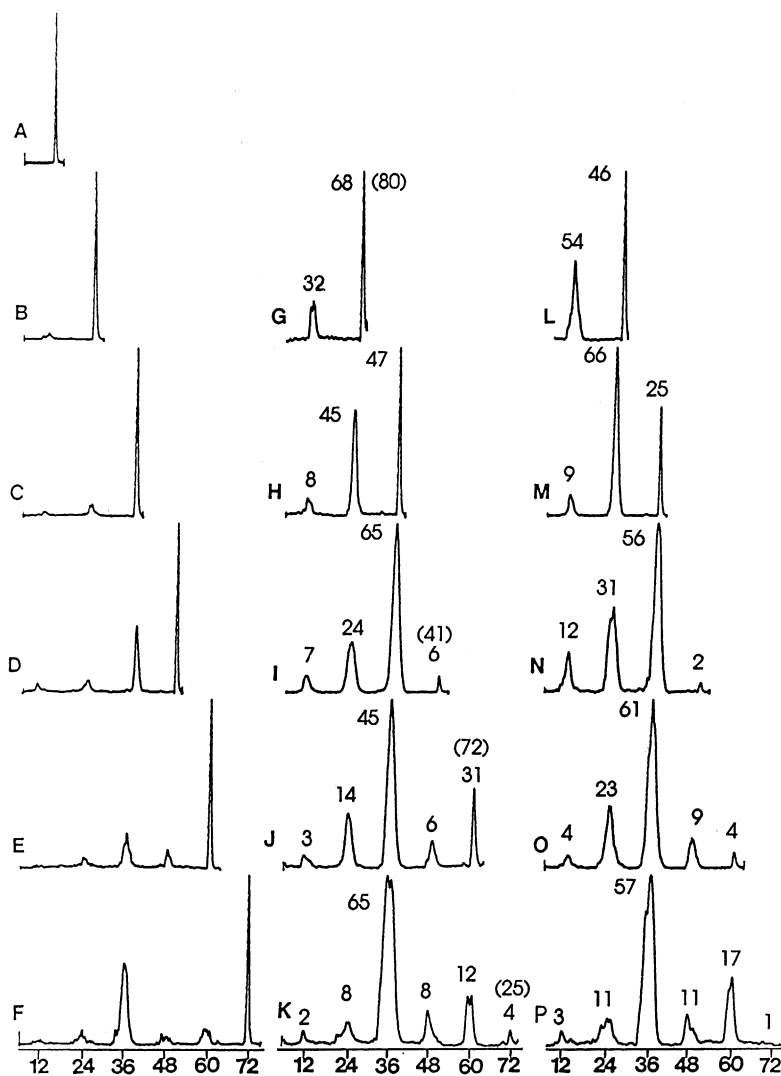


Fig. 3. ${}^+NR^+$ spectra, Y/O_2 (70%T), Y = neutralization target, identical ($\pm 10\%$) for the same ion from the listed precursors: (A) C_1^+ ; (B, G, L) C_2^+ ; (C, H, M) C_3^+ ; (D, I, N) C_4^+ ; (E, J, O) C_5^+ ; (F, K, P) C_6^+ ; with (A–F) $Y = Xe$ (70%T), (G–K) $Y = Na$ (85%T), (L–P) $Y = K$ (90%T). Precursors as in Fig. 1, except C_3^+ is from $n-C_3H_6$ and $n-C_4Cl_6$ and also from $c-C_3H_6$ and $c-C_5Cl_6$ with K neutralization; C_4^+ is from $n-C_4Cl_6$, $i-C_4H_7Br$, and $c-C_5Cl_6$ and also from $c-C_6Cl_6$ with Na and K neutralization. Numeric values for precursors are the percentage of the value with no collisions (value for Ca neutralization in parenthesis). Product values are relative peak areas, corrected for dissociation after reionization indicated in the Xe spectra, and averaged for the multiple measurements.

precursor peak, with fragment peak abundances closely similar to those in the corresponding CAD spectra. This is consistent with the formation of these fragments by dissociation of cations after reionization, not by neutral dissociation [59]. More excited neutrals can be formed by using a target of a lower ionization

energy (IE), thus removing less energy from the ion in the electron transfer process [60]. Using Na or K (IE = 5.14 or 4.34 eV) greatly reduced the reionized precursor peak for C_4 – C_6 (Fig. 3), consistent with a corresponding extent of neutral dissociation. However, the fragment relative abundances were still

independent (± 10) of the precursor molecule used for all C_n^+ ions studied.

The surviving precursor concentration from an intermediate extent of C_4^0 dissociation should yield a more sensitive test of isomeric identity than the relative abundances of the C_{1-3}^0 products, as dissociation could be preceded by isomerization of the C_4^0 precursor [11]. Neutralization with calcium (IE = 6.11 eV) did provide partial C_4^0 dissociation (Table 7), but $^+NR^+$ spectra from five different precursors still had closely similar abundances of reionized C_4^+ as well as C_{1-3}^+ fragment ions.

As a further test of the C_4^+ ion structure formed from a linear precursor, [1,4- $^{13}C_2$]-1,3-butadiene was used in an attempt to generate $^{13}C-^{12}C-^{12}C-^{13}C^+$. Its CAD (O_2 (70%T)) and NR (K (90%T)/ O_2 (70%T)) spectra showed intensity ratios for ($m/z = 24$):($m/z = 25$):($m/z = 26$) of 1.3:4.7:1 and 1.1:4.3:1, respectively, and ratios for ($m/z = 37$):($m/z = 38$) of 0.99:1 and 1.00:1, respectively. For these peak abundances, single bond dissociation of $^{13}C-^{12}C-^{12}C-^{13}C^+$ without isomerization would yield 0:1:0 and 1:0 ratios, respectively. By contrast, with complete scrambling, these ratios should be 1:4:1 and 1:1. Hence, the CAD and NR data indicate an almost complete scrambling of the carbon atoms. The scrambling may occur during ion formation by dissociative ionization, following neutralization, or upon collisional activation or reionization. Since the C_4^+ cations are formed by consecutive losses of several hydrogen or halogen atoms, it is possible that an ionic intermediate can undergo

an isomerization through cyclization and ring opening, thus scrambling the carbon atoms in the final carbon cluster. Isomerization in C_4^+ has been addressed recently by Blanksby et al. [11] who reported substantial ($\approx 75\%$) yet incomplete ^{13}C scrambling in $^{13}C-^{12}C-^{12}C-^{13}C^+$ produced by charge reversal from the anion. Scrambling further increased to $\approx 89\%$ upon neutralization of the anion followed by reionization of C_4^0 . Since stable C_4^- does not undergo carbon scrambling [11], the previous data indicated that the isomerization must have occurred in the cation and, to a lesser extent, in C_4^0 formed by collisional neutralization.

Similar to C_4^+ , the CAD (He (70%T)), NR (K (90%T)/ O_2 (70%T)) NR (K (90%T)/He (70%T)), and charge-reversal (C_6H_6 (30%T)) spectra of $^{12}C-^{13}C-^{12}C^+$ from propene-2- ^{13}C also showed substantial scrambling. The intensity ratios of ($m/z = 24$):($m/z = 25$) in these spectra were found to be 1:2.1, 1:2.0, 1:2.2, and 1:2.1, respectively; complete scrambling should give 1:2. This is consistent with the facile interconversion of linear and cyclic C_3^+ (vide supra) that should rapidly scramble the ^{13}C label in non-dissociating ions. Note that the lifetimes of C_3^+ submitted to CAD and NR were $\approx 20 \mu s$, which should provide sufficient time for carbon scrambling.

4.4. CAD and NR efficiencies

As reported earlier [4,25–27], the relative yields of C_n^+ in CAD spectra (Fig. 1) are consistent with the expected higher stability of the odd-numbered cationic clusters. The relative efficiencies for CAD of C_n^+ (Table 8) also reflect this stability relationship, assuming increasing dissociation cross section with increasing size, as found for metastable ion ($\approx 10^{-5}$ s lifetime) dissociations. Although mass discrimination [61] could affect the summed product cation abundances from CAD of C_n^+ , the value for C_7^+ is well below those of C_4^+ , C_5^+ , and C_6^+ . Metastable ion studies found a small [26] or significant [25] decrease in the cross section for C_7^+ versus C_6^+ , but still greater than the value for C_5^+ (C_4^+ was not measured). For ion–molecule reactions of laser-generated C_7^+ ions, two-thirds were found to be unreactive with

Table 7
 $^+NR^+$ spectra of C_4^+ , Ca($\sim 85\%$ T)/ O_2 (70%T)

Precursor	Relative abundance ^b			
	m/z			
	12	24	36	48
<i>n</i> -C ₄ H ₆	5	16	56	23
<i>n</i> -C ₄ Cl ₆	6	16	60	19
<i>c</i> -C ₅ Cl ₆	6	14	60	21
<i>c</i> -C ₆ H ₆	5	19	56	19
<i>c</i> -C ₆ Cl ₆	7	17	58	18

^a Transmittance from 690°C Ca vaporization.

^b % Relative to the sum of reionized ion intensities.

Table 8
Conversion efficiencies in CAD and NR spectra

Cluster	$C_n^+ \rightarrow C_{<n}^+$ ^a	$C_n^+ \rightarrow C_{\leq n}^0$ ^b	$C_n^+ \rightarrow C_{\leq n}^-$ ^c	$C_n^0 \rightarrow C_{\leq n}^+$ ^d	$C_n^- \rightarrow C_{<n}^-$ ^e
C ₁	–	15.4	0.40	5.2	–
C ₂	0.28	12.6	0.90	2.1	<1
C ₃	0.42	9.8	0.23	1.8	18
C ₄	1.8	7.7	0.24	0.90	25
C ₅	1.8	6.3	0.09	0.60	37
C ₆	2.8	4.9	0.14	0.30	20
C ₇	0.80	–	–	–	–

^a C_n^+ CAD, O₂ (50%T), efficiency: total C_n^+ product ion abundance in percentage of unattenuated precursor ion intensity ($\pm 20\%$ relative).

^b C_n^+ neutralization, Xe (70%T), efficiency: total $C_{\leq n}^0$ flux in percentage of unattenuated precursor ion intensity ($\pm 10\%$ relative).

^c C_n^+ charge reversal, C₆H₆ (30%T), efficiency: total $C_{\leq n}^-$ abundances in percentage of unattenuated precursor ion intensity ($\pm 20\%$ relative).

^d C_n^0 (from Xe (70%T) neutralization of C_n^+) reionization, O₂ (70%T), efficiency: total $C_{\leq n}^+$ abundances in percentage of unattenuated precursor ion intensity ($\pm 20\%$ relative).

^e C_n^- dissociation efficiency in charge reversal spectra, C₆H₆ (30%T): total $C_{<n}^-$ product ion abundances in percentage of survivor C_n^- .

D₂, indicating that the majority of ions have the cyclic structure [27]. The relatively low degree of fragmentation for $C_7^+ \rightarrow C_{<7}^+$ (Table 8) indicates that C_7^+ is unusually stable and/or of smaller physical cross section for undergoing collision. Either reason is consistent with a possibly higher fraction of cyclic isomers for C_7^+ prepared by dissociative ionization of cyclic precursors. As a corollary, this also implies that C₅⁺ and C₆⁺ are mainly the linear isomers. For the even-numbered, less stable C₄⁺ and C₆⁺ clusters, the increase in $C_n^+ \rightarrow C_{\leq n}^+$ CAD efficiencies should be due primarily to increasing size, consistent also with a linear structure for C₄⁺.

The $C_n^+ \rightarrow C_{\leq n}^+$ neutralization efficiency (Table 8) decreases quite regularly from C₁ (15.4%) to C₆ (4.9%); the increasing physical cross section apparently is more effective in producing scattering than electron transfer. The $C_n^0 \rightarrow C_{\leq n}^+$ reionization efficiency decreases even more dramatically from C₁ (5.2%) to C₆ (0.3%) despite decreasing IE values. Neither the $C_n^+ \rightarrow C_n^+$ nor $C_n^0 \rightarrow C_n^+$ efficiencies reflect the odd/even nature of the cluster, consistent with the fact that odd clusters are more stable for both C_n^0 and C_n^+ . In contrast, the efficiency of forming C_n^- from C_n^+ favors the even-numbered clusters. Although the efficiency for $C_n^+ \rightarrow C_n^-$ drops substantially from C₂ (0.90%) to C₆ (0.14%), most of

this effect appears to be due to the drop in neutralization efficiency, $C_n^+ \rightarrow C_n^0$, which follows the same trend. The negative effect of cluster size should be far less for $C_n^0 \rightarrow C_n^-$ than for the highly endothermic $C_n^0 \rightarrow C_n^+$ process.

4.5. Dissociation energetics

The thermochemical data inferred from experimental and computational studies were checked to predict competitive product formation upon unimolecular dissociations following neutralization (Fig. 3). This assumes minimal entropy requirements, and kinetic energy release measurements for C_n^+ metastable ion dissociations indicate negligible reverse activation energy [25,26]. It should be noted that these comparisons can only be qualitative, because of serious mass discrimination against smaller product ions. For example, on the basis of ion dissociation energies (Table 6), [C₁⁺] in the C₃⁺ NR spectrum (Fig. 3) should be more abundant than [C₂⁺]. However, the smaller C_n^0 products are expected to be scattered more efficiently when excess excitation energy is converted to the kinetic energy of products. Offsetting this somewhat, the smaller C_n^0 fragments have higher reionization efficiencies (Table 8), and their abundances are also increased by secondary

product dissociation, as shown by K and Na NR spectra.

For C_n^0 NR data (Fig. 3 and Table 7), formation of $\{C_1^0 + C_3^0\}$ is favored over that of $2C_2^0$. This agrees with the dissociation energies for both neutral and cationic dissociations. For the former, our calculations predict $\{C_1^0 + C_3^0\}$ formation to be 124 kJ/mol less endothermic than $2C_2$. This is corroborated by the revised enthalpies of formation [37] of the dissociation products (Table 9) that prefer $\{C_1^0 + C_3^0\}$ by 92 kJ/mol. Post-reionization C_4^+ dissociations also prefer $\{[C_1^0] + [C_3^+]\}$ and $\{[C_1^+] + [C_3^0]\}$ over $\{[C_2^0] + [C_2^+]\}$ by 119 and 173 kJ/mol, respectively. For C_5^0 dissociation, the formation of $\{C_2^0 + C_3^0\}$ is

favored over $\{C_1^0 + C_4^0\}$ by 115 and 96 kJ/mol from experiment and theory, respectively, which is reflected by the spectra (Fig. 3). For C_6^0 dissociation, the thermochemical data prefer formation of $2C_3^0$, followed by $\{C_1^0 + C_5^0\}$, and $\{C_2^0 + C_4^0\}$. This ordering is consistent with the relative abundances of products in the Na and K $^+NR^+$ spectra of C_6^0 (Fig. 3).

The $^+NR^-$ spectra of C_n^+ (Fig. 2) show substantially less dissociation than those from $^+NR^+$. In part this is due to less excitation in intermediate C_n^0 upon electron transfer from benzene (IE = 9.25 eV [35]). In addition, both theory and experiment predict highly endothermic dissociations of C_n^- (Table 6). Most dissociation energies exceed the electron affinity of the C_n^- , so that energized anions can be expected to autodetach an electron (and become undetectable in the mass spectra) rather than dissociate on the anion potential energy surface. This implies that the dissociations observed in the $^+NR^-$ can be assigned to a small fraction of energetic C_n^0 of above-threshold internal energies. The product distribution qualitatively follows that observed in the Na and K $^+NR^+$; the main dissociations are $C_4^0 \rightarrow \{C_3^0 + C_1^0\}$, $C_5^0 \rightarrow \{C_3^0 + C_2^0\}$ and $C_6^0 \rightarrow \{C_3^0 + C_3^0\}$ corresponding to lowest threshold energies.

Table 9

Enthalpies of formation of C_n^0 , C_n^+ , and C_n^-

Species	$\Delta H_{f,0}^{a,b}$		
	B3LYP	CCSD(T)	Experimental ^c
Neutrals			
C_1^0	–	–	711
C_2^0	920	834	817
C_3^0	699	830	831
C_4^0	846	1049	1052
C_5^0	–	–	1081
C_6^0	–	–	1312
Cations			
C_1^+	1824	1790	1797
C_2^+	2058	1972	1967
C_3^+	1878	1967	1902–1998
C_4^+	1889	2093	<2302
C_5^+	–	–	<2264
C_6^+	–	–	2248
Anions			
C_1^-	579	593	589
C_2^-	499	527	502
C_3^-	605	642	639
C_4^-	669	687 ^d	677
		812 ^e	–
C_5^-	–	–	807
C_6^-	–	–	908

^aAt 0 K in units of kJ/mol.

^bFrom the calculated enthalpies of formation, ionization energies, and electron affinities.

^cFrom experimental enthalpies of formation ([37] unless stated otherwise), ionization energies, and electron affinities.

^dFrom $(^3\Sigma_g^-)C_4^0 \rightarrow (^2\Pi_g^-)C_4^-$.

^eFrom $(^1A_g)C_4^0 \rightarrow (^2B_{2g})C_4^-$.

4.6. NR energy deposition

Neutralization of C_n^+ with alkali metal targets deposits substantial internal energy into the neutral clusters formed. This can be approximated by $E^* \leq IE(C_n^0) - IE(\text{target})$, with target IE(Ca, Na, K) = 6.11, 5.14, and 4.34 eV. An additional vibrational energy can be deposited through Franck–Condon effects due to a mismatch of the ion and neutral potential energy surfaces [62]. Although Franck–Condon effects >100 kJ/mol have been reported for collisional electron transfer in some systems [63], much smaller effects can be expected for $C_n^+ \rightarrow C_n^0$ where the differences between the ion and neutral geometries are mostly small (Table 1).

The neutralization of C_3^+ by Na (K) should produce C_3^0 with $E^* = 6.1$ (6.9) eV. This causes 53% (75%) C_3^0 dissociation that requires 7.22 eV (697 kJ/mol) at

the thermochemical threshold (Table 6). Note that stable C_3^+ precursors may contain up to 542 kJ/mol internal energy (lowest ion dissociation threshold, Table 6), which, when combined with the energy acquired upon neutralization, can provide the excitation energy for dissociation. However, comparison of the Xe (negligible excitation upon neutralization) and Na (K) NR spectra (Fig. 3) clearly shows that the energy due to exothermic electron transfer has the predominant effect on cluster dissociation.

Neutralization of the most stable ($^2A'$) C_4^+ by Ca, Na, and K should produce (1A_g) C_4^0 with 4.71, 5.68, and 6.48 eV, respectively. For Ca neutralization this results in 77–82% dissociation, for Na and K the dissociation is >95% complete. The dissociation thresholds in (1A_g) C_4^0 are 4.78 and 6.06 eV to form $\{C_1^0 + C_3^0\}$ and $\{C_2^0 + C_2^0\}$, respectively, (Table 6), consistent with the dissociations observed on NR. Likewise, dissociations of C_5^0 and C_6^0 are greatly enhanced by exothermic neutralization with Na and K (Fig. 3). An exception is C_2^0 for which is only 32% dissociated in spite that Na (K) neutralization should deposit 6.66 (7.46) eV to overcome the 605 kJ/mol dissociation threshold (Table 6). The excited electronic states of the small C_2^0 molecule have well-separated energies [4,5,46] and thus could have sufficiently long lifetimes (>0.5 μ s) to reach the reionization cell before dissociation.

5. Conclusions

Although multiple isomeric C_3^0 and C_4^0 species are predicted to be stable, those prepared from a wide variety of linear, branched, and cyclic (and isotopically labeled) precursors give NR spectra indicative of only one isomer or common mixtures. This is consistent with the present theoretical calculations that point to facile interconversion of C_3^+ , and with a recent study by Blanksby et al. [11] on equilibration of linear and cyclic C_4^+ and C_4^0 . While most of the calculated enthalpies of formation, ionization energies, and electron affinities agree well with currently accepted experimental data, a substantial discrepancy still exists

between the calculated and experimental ionization energies of C_3^0 and C_4^0 [57] that should be revisited.

Acknowledgements

We appreciate initial studies by C. Wesdemiotis and M.-Y. Zhang, samples from W.T. Miller, helpful discussions with M.T. Bowers, D.E. Drinkwater, J.R. Eyler, C. Lifshitz, K. Raghavachari, M.M. Ross, and C.L. Wilkins, and the generous financial support of the Office of Naval Research (Grant No. M00014-90-J-1948) and, for instrumentation the National Science Foundation (Grant No. CHE-9014883), and the National Institutes of Health (Grant No. GM-16609). Computations at the University of Washington Computational Chemistry Center were jointly supported by the NSF (Grant No. CHE-9808182) and University of Washington.

References

- [1] (a) G. Herzberg, *Astrophysics* 96 (1942) 314; (b) P.F. Bernath, *Science* 244 (1989) 562.
- [2] H.W. Kroto, *Science* 242 (1988) 1139.
- [3] (a) O. Hahn, F. Strassman, J. Mattauich, H. Ewald, *Naturwiss* 30 (1942) 541; (b) W.A. Chupka, M.G. Inghram, *J. Chem. Phys.* 22 (1954) 1472.
- [4] (a) D.M. Cox, K.C. Reichmann, A. Kaldor, *J. Chem. Phys.* 88 (1988) 1588; (b) W. Weltner Jr., R.J. Vanzee, *Chem. Rev.* 89 (1989) 1713; (c) J.R. Heath, *Spectroscopy* 5 (1990) 36.
- [5] J.M.L. Martin, J.P. Francois, R. Gijbels, *J. Comput. Chem.* 12 (1991) 52.
- [6] (a) J.E. Campana, *Mass Spectrom. Rev.* 6 (1987) 395; (b) R.F. Curl, R.E. Smalley, *Science* 242 (1988) 1017; (c) S.W. McElvany, *J. Chem. Phys.* 89 (1988) 2063.
- [7] (a) J.L. Robertson, S.C. Moss, Y. Lifshitz, S.R. Kasi, J.W. Rabalais, G.D. Lempert, E. Rapaport, *Science* 243 (1989) 1047; (b) W.A. Yarbrough, R. Messier, *Science* 247 (1990) 688.
- [8] H.W. Kroto, *J. Chem. Soc., Faraday Trans.* 86 (1990) 2465.
- [9] P. Freivogel, M. Grutter, D. Forner, J.P. Maier, *Chem. Phys. Lett.* 249 (1996) 191.
- [10] A. Fura, F. Turecek, F.W. McLafferty, *ONR Report* (1993); *Chem. Abstr.* 124 (1995) 8103.
- [11] S.J. Blanksby, D. Schroder, S. Dua, J.H. Bowie, H. Schwarz, *J. Am. Chem. Soc.* 122 (2000) 7105.
- [12] S. Dua, J.H. Bowie, Presented at the 18th ANZMS Conference, Gold Coast, Australia, February 2001.

- [13] (a) P.O. Danis, C. Wesdemiotis, F.W. McLafferty, *J. Am. Chem. Soc.* 105 (1983) 7454;
(b) D.V. Zagorevski, J.L. Holmes, *Mass Spectrom. Rev.* 18 (1999) 87.
- [14] K.S. Pitzer, E. Clementi, *J. Am. Chem. Soc.* 81 (1959) 4477.
- [15] (a) K. Raghavachari, J.S. Binkley, *J. Chem. Phys.* 87 (1987) 2191;
(b) K. Raghavachari, *Z. Phys. D* 12 (1989) 61.
- [16] L. Adamowicz, *J. Chem. Phys.* 94 (1991) 1241.
- [17] (a) P.R. Taylor, J.M.L. Martin, J.P. Francois, R. Gijbels, *J. Phys. Chem.* 95 (1991) 6530;
(b) R.S. Grev, I.L. Alberts, H.F. Schaefer III, *J. Phys. Chem.* 94 (1990) 3379;
(c) K. Raghavachari, *Chem. Phys. Lett.* 171 (1990) 249;
(d) J.M.L. Martin, J.-P. Francois, R. Gijbels, *J. Chem. Phys.* 93 (1990) 5037;
(e) G.E. Scuseria, *Chem. Phys. Lett.* 176 (1991) 27.
- [18] (a) J.M.L. Martin, J.-P. Francois, R. Gijbels, *J. Chem. Phys.* 94 (1991) 3753;
(b) G. Pacchioni, J. Koutecky, *J. Chem. Phys.* 88 (1988) 1066.
- [19] J.D. Watts, J. Gauss, J.F. Stanton, R.J. Bartlett, *J. Chem. Phys.* 97 (1992) 8372.
- [20] J.M.L. Martin, P.R. Taylor, *J. Chem. Phys.* 102 (1995) 8270.
- [21] J.M.L. Martin, J. El-Yazel, J.-P. Francois, *Chem. Phys. Lett.* 242 (1995) 570.
- [22] S. Schmatz, P. Botschwina, *Int. J. Mass Spectrom. Ion Processes* 149/150 (1995) 621.
- [23] M.G. Giuffreda, M.S. Deleuze, J.-P. Francois, *J. Phys. Chem.* 103 (1999) 5137.
- [24] (a) M.J. Deluca, M.A. Johnson, *Chem. Phys. Lett.* 152 (1988) 67;
(b) A.N. Pargellis, *J. Chem. Phys.* 93 (1990) 2099.
- [25] (a) P.P. Radi, T.L. Bunn, P.R. Kemper, M.E. Molchan, M.T. Bowers, *J. Chem. Phys.* 88 (1988) 2809;
(b) P.P. Radi, M.E. Rincon, M.T. Hsu, J. Brodbelt-Lustig, P.R. Kemper, M.T. Bowers, *J. Phys. Chem.* 93 (1989) 6187.
- [26] (a) C. Lifshitz, T. Peres, S. Kababia, I. Agranat, *Int. J. Mass Spectrom. Ion Processes* 82 (1988) 193;
(b) C. Lifshitz, T. Peres, I. Agranat, *Int. J. Mass Spectrom. Ion Processes* 93 (1989) 149;
(c) C. Lifshitz, P. Sandler, H.-F. Grutzmacher, J. Sun, T. Weiske, H. Schwarz, *J. Phys. Chem.* 97 (1993) 6592;
(d) J. Sun, H.-F. Grutzmacher, C. Lifshitz, *J. Am. Chem. Soc.* 115 (1993) 8382.
- [27] (a) S.W. McElvany, B.I. Dunlap, A. O'Keefe, *J. Chem. Phys.* 86 (1987) 715;
(b) D.C. Parent, S.W. McElvany, *J. Am. Chem. Soc.* 111 (1988) 2393;
(c) S.B.H. Bach, J.R. Eyler, *J. Chem. Phys.* 92 (1990) 358.
- [28] S. Yang, K.J. Taylor, M.J. Craycraft, J. Conceicao, C.L. Pettiette, O. Cheshnovsky, R.E. Smalley, *Chem. Phys. Lett.* 144 (1988) 431.
- [29] (a) J. Szczepanski, R. Hodyss, M. Vala, *J. Phys. Chem. A* 102 (1998) 8300;
(b) J. Szczepanski, S. Ekern, M. Vala, *J. Phys. Chem. A* 101 (1997) 1841;
(c) J. Szczepanski, C. Wehlburg, M. Vala, *J. Phys. Chem. A* 101 (1997) 7039;
(d) M. Miki, T. Wakabayashi, T. Momose, T. Shida, *J. Phys. Chem.* 100 (1996) 12135;
(e) R.H. Kranze, W.R.M. Graham, *J. Chem. Phys.* 96 (1992) 2517;
(f) J. Szczepanski, R. Pellow, M. Vala, *Z. Naturforsch. A: Phys. Sci.* 47 (1992) 595;
(g) J. Almlöf, P. Jensen, F.J. Northrup, C.M. Rohlffing, E.A. Rohlffing, T.J. Sears, *J. Chem. Phys.* 101 (1994) 5413;
(h) J. Szczepanski, M. Vala, *J. Chem. Phys.* 99 (1993) 7371;
(i) L.N. Shen, W.R.M. Graham, *J. Chem. Phys.* 91 (1989) 5115;
(j) P.F. Bernath, K.H. Hinkle, J.J. Keady, *Science* 244 (1989) 562;
(k) M. Vala, T.M. Chandrasekhar, J. Szczepanski, R.J. Van Zee, W. Weltner Jr., *J. Chem. Phys.* 90 (1989) 595;
(l) J.R. Heath, A.L. Cooksy, M.H.W. Gruebele, C.A. Schmuttenmaer, R.J. Saykally, *Science* 244 (1989) 564;
(m) J.R. Heath, R.A. Sheeks, A.L. Cooksy, R.J. Saykally, *Science* 249 (1990) 895;
(n) L.N. Shen, P.A. Withey, W.R.M. Graham, *J. Chem. Phys.* 88 (1988) 3465.
- [30] R.J. Van Zee, R.F. Ferrante, K.J. Zeringue, W. Weltner Jr., *J. Chem. Phys.* 88 (1988) 3465.
- [31] (a) G. von Helden, M. Hsu, P.R. Kemper, M.T. Bowers, *J. Chem. Phys.* 95 (1991) 3835;
(b) G. von Helden, P.R. Kemper, N.G. Gotts, M.T. Bowers, *Science* 259 (1993) 1300;
(c) M.T. Bowers, P.R. Kemper, G. von Helden, P.A.N. van Koppen, *Science* 260 (1993) 1446.
- [32] (a) A. Faibis, E.P. Kanther, L.M. Tack, E. Bakke, B.J. Zabransky, *J. Phys. Chem.* 91 (1987) 6445;
(b) M. Algranati, H. Feldman, D. Kella, E. Malkin, E. Miklazky, R. Naaman, Z. Vager, Z. Zajfman, *J. Chem. Phys.* 90 (1989) 4617;
(c) H. Feldman, D. Kella, E. Malkin, E. Miklazky, Z. Vager, J. Zajfman, R. Naaman, *J. Chem. Soc., Faraday Trans.* 86 (1990) 2469.
- [33] D. Zajfman, H. Feldman, O. Heber, D. Kella, D. Majer, Z. Vager, R. Naaman, *Science* 258 (1992) 1129.
- [34] M. Vala, T.M. Chandrasekhar, J. Szczepanski, R. Pellow, *J. Mol. Struct.* 222 (1990) 209.
- [35] (a) S.G. Lias, J.E. Bartmess, J.F. Liebman, J.L. Holmes, R.D. Levin, W.G. Mallard, *J. Phys. Chem. Ref. Data* 17 (Suppl. 1) (1988).;
(b) NIST Standard Reference Database No. 69, February 2000 Release (<http://webbook.nist.gov/chemistry>).
- [36] R. Ramanathan, J.A. Zimmerman, J.R. Eyler, *J. Chem. Phys.* 98 (1993) 7838.
- [37] K.A. Gingerich, H.C. Finkbeiner, R.W. Schmude, *J. Am. Chem. Soc.* 116 (1994) 3884.
- [38] (a) R. Feng, C. Wesdemiotis, M.A. Baldwin, F.W. McLafferty, *Int. J. Mass Spectrom. Ion Processes* 86 (1988) 96;
(b) D.E. Drinkwater, A. Fura, M.-Y. Zhang, F.W. McLafferty, *Org. Mass Spectrom.* 26 (1991) 1032;

- (c) D.E. Drinkwater, F. Turecek, F.W. McLafferty, *Org. Mass Spectrom.* 26 (1991) 559.
- [39] A.B. Susan, W.P. Duncan, *J. Lab. Comp. Radiochem.* XVIII (8) (1985) 1227.
- [40] M.J. Frisch, G.W. Trucks, H.B. Schlegel, G.E. Scuseria, M.A. Robb, J.R. Cheeseman, V.G. Zakrzewski, J.A. Montgomery Jr., R.E. Stratmann, J.C. Burant, S. Dapprich, J.M. Millam, A.D. Daniels, K.N. Kudin, M.C. Strain, O. Farkas, J. Tomasi, V. Barone, M. Cossi, R. Cammi, B. Mennucci, C. Pomelli, C. Adamo, S. Clifford, J. Ochterski, G.A. Petersson, P.Y. Ayala, Q. Cui, K. Morokuma, D.K. Malick, A.D. Rabuck, K. Raghavachari, J.B. Foresman, J. Cioslowski, J.V. Ortiz, B.B. Stefanov, G. Liu, A. Liashenko, P. Piskorz, I. Komaromi, R. Gomperts, R.L. Martin, D.J. Fox, T. Keith, M.A. Al-Laham, C.Y. Peng, A. Nanayakkara, C. Gonzalez, M. Challacombe, P.M.W. Gill, B. Johnson, W. Chen, M.W. Wong, J.L. Andres, C. Gonzalez, M. Head-Gordon, E.S. Replogle, J.A. Pople, *Gaussian 98*, Revision A.6, Gaussian, Inc., Pittsburgh, PA, 1998.
- [41] (a) A.D. Becke, *J. Chem. Phys.* 98 (1993) 1372, 5648.;
(b) P.J. Stephens, F.J. Devlin, C.F. Chabalowski, M.J. Frisch, *J. Phys. Chem.* 98 (1994) 11623.
- [42] T.H. Dunning Jr., *J. Chem. Phys.* 90 (1989) 1007.
- [43] J. Cizek, *J. Adv. Chem. Phys.* 14 (1969) 35.
- [44] G.D. Purvis, R.J. Bartlett, *J. Chem. Phys.* 76 (1982) 1910.
- [45] (a) H.B. Schlegel, *J. Chem. Phys.* 84 (1986) 4530;
(b) I. Mayer, *Adv. Quantum Chem.* 12 (1980) 189.
- [46] (a) C. Petrongolo, P.J. Bruna, S.D. Peyerimhoff, R.J. Buenker, *J. Chem. Phys.* 74 (1981) 4594;
(b) P. Rosmus, H.-J. Werner, E.-A. Rensch, M. Larsson, *J. Electron Spectrosc. Relat. Phenom.* 41 (1986) 289.
- [47] H. Hotop, W.C. Lineberger, *J. Phys. Chem. Ref. Data* 14 (1985) 731.
- [48] D.W. Arnold, S.E. Bradforth, T.N. Kitsopoulos, D.M. Neumark, *J. Chem. Phys.* 95 (1991) 8753.
- [49] K.M. Ervin, S. Gronert, S.E. Barlow, M.K. Gilles, A.G. Harrison, V.M. Bierbaum, W.C. Lineberger, *J. Am. Chem. Soc.* 112 (1990) 5750.
- [50] J.M. Oakes, G.B. Ellison, *Tetrahedron* 42 (1986) 6263.
- [51] S. Yang, K.J. Taylor, M.J. Craycraft, J. Conceicao, C.L. Pettiette, O. Chervonovskiy, R.E. Smalley, *Chem. Phys. Lett.* 144 (1989) 431.
- [52] C.J. Reid, J.A. Ballantine, S.R. Andrews, F.M. Harris, *Chem. Phys.* 190 (1995) 113.
- [53] P. Plessis, P. Marmet, *Int. J. Mass Spectrom. Ion Processes* 70 (1986) 23.
- [54] K.P. Huber, G. Herzberg, *Molecular Spectra and Molecular Structure. IV. Constants of Diatomic Molecules*, Van Nostrand Reinhold, New York, 1979, p. 1.
- [55] S.K. Gupta, K.A. Gingerich, *J. Chem. Phys.* 71 (1979) 3072.
- [56] J.R. Wyatt, F.E. Stafford, *J. Phys. Chem.* 76 (1972) 1913.
- [57] R. Ramathan, J.A. Zimmerman, J.R. Eyler, *J. Chem. Phys.* 98 (1993) 7838.
- [58] (a) R. Feng, C. Wesdemiotis, M.-Y. Zhang, M. Marchetti, F.W. McLafferty, *J. Am. Chem. Soc.* 111 (1989) 1986;
(b) M.-Y. Zhang, C. Wesdemiotis, M. Marchetti, P.O. Danis, J.C. Ray, B.K. Carpenter, F.W. McLafferty, *J. Am. Chem. Soc.* 113 (1989) 8341.
- [59] F.W. McLafferty, C. Wesdemiotis, *Org. Mass Spectrom.* 24 (1989) 663.
- [60] (a) G.I. Gellene, R.F. Porter, *Acc. Chem. Res.* 16 (1983) 200;
(b) M. Abshagen, J. Kowalski, M. Meyberg, G.Z. Pulitz, F. Trager, J. Well, *Europhys. Lett.* 5 (1988) 13.
- [61] R.A. Chorush, I. Vidavsky, F.W. McLafferty, *Org. Mass Spectrom.* 28 (1993) 1016.
- [62] V.Q. Nguyen, F. Turecek, *J. Mass Spectrom.* 31 (1996) 843.
- [63] (a) F. Turecek, M. Gu, C.E.C.A. Hop, *J. Phys. Chem.* 99 (1995) 2278;
(b) V.Q. Nguyen, F. Turecek, *J. Mass Spectrom.* 31 (1996) 1173.